Temporal summation in myopia and its implications for the investigation of glaucoma

Link to publication record in Ulster University Research Portal

Document Version
Publisher's PDF, also known as Version of record

ORIGINAL ARTICLE

OPO — THE COLLEGE OF OPTOMETRISTS

Temporal summation in myopia and its implications for the investigation of glaucoma

Victoria Stapley[1] | Roger S. Anderson[1,2] | Tony Redmond[3] | Kathryn Saunders[1] | Pádraig J. Mulholland[1,2]

[1]Centre for Optometry & Vision Science, Biomedical Sciences Research Institute, Ulster University, Coleraine, UK

[2]National Institute for Health & Care Research (NIHR) Biomedical Research Centre at Moorfields Eye Hospital NHS Foundation Trust and UCL Institute of Ophthalmology, London, UK

[3]School of Optometry and Vision Sciences, Cardiff University, Cardiff, Maindy Road, UK

Correspondence
Victoria Stapley, Centre for Optometry & Vision Science, Biomedical Sciences Research Institute, Ulster University, Coleraine, Northern Ireland, UK.
Email: v.stapley@ulster.ac.uk

Abstract

Purpose: We have previously demonstrated the upper limit of complete spatial summation (Ricco's area) to increase in non-pathological axial myopia compared to non-myopic controls. This study sought to investigate whether temporal summation is also altered in axial myopia to determine if this aspect of visual function, like in glaucoma, is influenced by reductions in retinal ganglion cell (RGC) density.

Methods: Achromatic contrast thresholds were measured for a GIII-equivalent stimulus (0.43° diameter) of six different stimulus durations (1–24 frames, 1.1–187.8 ms) in 24 participants with axial myopia (mean spherical refractive error: −4.65D, range: −1.00D to −11.25D, mean age: 34.1, range: 21–57 years) and 21 age-similar non-myopic controls (mean spherical refractive error: +0.87D, range: −0.25D to +2.00D, mean age: 31.0, range: 18–55 years). Measurements were performed at 10° eccentricity along the 90°, 180°, 270° and 360° meridians on an achromatic 10 cd/m^2 background. The upper limit of complete temporal summation (critical duration, CD) was estimated from the data with iterative two-phase regression analysis.

Results: There was no significant difference ($p = 0.90$, Mann–Whitney U-test) in median CD between myopes (median: 44.3 ms; IQR: 26.5, 51.2) and non-myopes (median: 41.6 ms; IQR: 27.3, 48.5). Despite RGC numbers underlying the stimulus being significantly lower in the myopic group ($p < 0.001$), no relationship was observed between the CD estimate and co-localised RGC number (Pearson's $r = -0.13$, $p = 0.43$) or ocular length (Pearson's $r = -0.08$, $p = 0.61$).

Conclusions: Unlike spatial summation, temporal summation is unchanged in myopia. This contrasts with glaucoma where both temporal and spatial summation are altered. As such, perimetric methods optimised to test for anomalies of temporal summation may provide a means to differentiate between conditions causing only a reduced RGC density (e.g., myopia), and pathological processes causing both a reduced RGC density *and* RGC dysfunction (e.g., glaucoma).

KEYWORDS
critical duration, myopia, perimetry, temporal summation

INTRODUCTION

It is well recognised that visual function is reduced in myopia. For example, measures of spatial vision including high-contrast visual acuity,[1,2] peripheral resolution acuity[3–5] and contrast sensitivity[6] have been reported to be reduced in non-pathological myopia. Recently, our group has also demonstrated an enlarged area of complete spatial summation (Ricco's area, RA) in axial myopia when inter-individual differences in retinal image size are accounted

for.[7] Such changes in spatial visual function in myopia have been attributed to the reduction in the density (cells/mm^2) of photoreceptors and retinal ganglion cells (RGCs) that results from axial elongation of the myopic eye.[2,4,7–9] Alterations in the structure and/or function of higher visual centres,[10–12] in addition to the concentration of circulating dopamine and dopamine antagonists,[7,13] have also been hypothesised to underpin such changes.

While many studies have investigated spatial vision in myopia, few have considered the effects on temporal vision, and those that did examine this effect have presented conflicting findings. For example, while Ong and Wong[14] and Chen et al.[15] reported a reduction in the critical flicker frequency (CFF) in high myopia, Comerford et al.[16] failed to observe any effect of high myopia on the temporal contrast sensitivity function for photopic, mesopic or scotopic luminance levels. Vera-Diaz et al.[17] also found no significant difference in monocular temporal contrast sensitivity between myopes and non-myopic controls but did report reduced stereopsis in myopes with flickering stimuli. Controversy also exists with regard to whether myopia affects the timing of the electroretinogram; some authors have found minimal[18–21] or no[22–26] changes, whereas others have reported delayed implicit times in myopia.[3,27–32] To our knowledge no study has examined temporal summation in non-pathological myopia.

Given that spatial summation is altered in myopia, the known interactions between spatial and temporal summation,[33] and the fact that anomalies of spatial summation can be accompanied by anomalies of temporal summation where RGC density is reduced in retinal disease,[34,35] it might reasonably be hypothesised that temporal summation is also altered in myopia. Complete temporal summation describes the reciprocal relationship between stimulus duration and stimulus contrast at threshold, such that $intensity \times duration = k$ (Bloch's law).[36] Bloch's law holds for short-duration stimuli up to a critical duration (CD). This is analogous to Ricco's law of complete summation in the spatial domain. For durations longer than the CD, the reciprocal relationship progressively breaks down until eventually thresholds become independent of duration; this point is known as the utilisation time.[37]

Previous studies have reported a longer CD with reduced background intensity[38] in glaucoma.[34,35] The findings of Barlow[38] of changes to CD (alongside changes to RA) with background luminance, are likely a physiological mechanism of the visual system to optimise visual function within a range of visual environments. A similar hypothesis was proposed by Mulholland et al. for the pathological processes in glaucoma, that is, both spatial and temporal summation are altered in compensation for RGC death and/or pre-morbid RGC dysfunction. Such changes would serve to maintain a constant signal-to-noise ratio, increasing overall neural sensitivity at the expense of spatial and temporal resolution.[35,39] In myopia, axial elongation and retinal stretch result in a sparser array of visual neurons. Such structural changes are also hypothesised to induce

---

Key points

- This study found that the limit of complete temporal summation (critical duration) is not altered in physiological myopia.
- Considering the findings in conjunction with published research on spatial summation in myopia, reduced visual function in physiological myopia likely results from increased retinal ganglion cell spacing rather than dysfunction.
- Unlike glaucoma, temporal summation is unaffected in myopia, suggesting that temporal summation deficits are a biomarker specific to glaucoma, and may aid cross-sectional differentiation between the two conditions.

---

damage to the retinal neurons, thereby compromising their normal function.[4,5,9,40] We hypothesise that the degree of both spatial and temporal summation within the myopic visual system may increase concurrently, as in glaucoma, to compensate for these structural and/or functional changes.

The primary aim of this study was to determine whether the CD is significantly different in axial myopes compared to non-myopic controls. The relationship between CD and co-localised measures of retinal structure (eye length, RGC number) was also investigated. Given recent evidence from electrophysiology measures that retinal signalling may be altered in myopia,[41] it is possible that alterations in temporal summation, a feature that is at least, in part, determined by neural processing at a retinal level,[35,42,43] may also occur in myopia. The measurement of temporal visual function in myopia may help determine whether myopia-associated axial elongation and retinal stretch are accompanied by neural damage. Clinically, an understanding of spatial and temporal summation, and any changes therein, are also important for informing more accurate and precise stimulus design in visual field assessment, given that changes in RA and CD are biomarkers for glaucoma.[35,39] Thus, knowledge of whether, or how, temporal summation changes in myopia will mean that detection of glaucoma may be less affected by confounding factors arising from the simultaneous presence of myopia. Finally, findings in myopia (regardless of whether there are changes in CD or not) are important for understanding the differential effects of RGC density and damage in glaucoma.

METHODS

Participants

Twenty-four participants with physiological axial myopia (median age 29.0, interquartile range 24.5–40.5 years) and twenty-one age-similar non-myopic controls (median age

25.0, IQR 22–39 years) were recruited for this study. We excluded pathological myopia (defined as high myopia with fundus abnormalities such as myopic macular degeneration and glaucoma[44]) through a strict screening protocol. Firstly, all participants were required to have best corrected (unaided or with their habitual spectacle correction) monocular, distance visual acuity of 0.00 logMAR (6/6) or better in both eyes. A detailed ocular examination was carried out by an experienced optometrist to rule out signs of myopic macular degeneration (chorioretinal atrophy, lacquer cracks, choroidal neovascularisation) or glaucoma. In addition, all participants had full visual fields, measured with the 24-2 SITA Standard threshold test (Humphrey Visual Field Analyser, Carl Zeiss Meditec, zeiss.com) and intraocular pressure was ≤21 mmHg as measured using Goldmann applanation tonometry. Peripapillary retinal nerve fibre layer (RNFL) and macular optical coherence tomography (OCT) scans (30°×25° rectangular patch, 61 B-scans, automatic real-time tracking (ART) 9, tilted to account for fovea-optic nerve axis) revealed no abnormalities (Spectralis OCT, Heidelberg Engineering GmbH., heidelberg engineering.com). The clinical examination also identified no media opacities or other concurrent ophthalmic disease. No participant had any systemic condition or was taking any medications known to affect vision.

Refractive error was classified using objective measurements taken with a binocular open-field autorefractor (Shin Nippon NVision-K 5001, grandseiko.com), at least 20 min after the instillation of tropicamide hydrochloride 1.0%. Three measurements were taken for each participant and the average was calculated and expressed as best vision sphere (BVS). Myopia was defined as BVS refractive error <−0.50 DS, and high myopia as <−5.00 DS.[44] Refractive errors ranged from −1.00 DS to −11.25 DS (median −4.59 DS) in the myopic group (including 12 participants [50%] with high myopia), and from −0.25 DS to +2.00 DS (median +1.00 DS) in the control group. Astigmatism was <3.00 DC in the test eye. The characteristics of each group are displayed in Table 1. Experiments were carried out on one eye only. If both eyes met the inclusion criteria, then the right eye was used.

Ethical approval for the study was granted by Ulster University, Biomedical Sciences Research Ethics Filter Committee. The research adhered to the tenets of the Declaration of Helsinki and informed, written consent was obtained from each participant prior to data collection.

Apparatus and stimuli

All psychophysical tests were undertaken on a gamma-corrected cathode ray tube (CRT) display (SONY 420GS; Sony Corp., sony.net; pixel resolution 1280×1024, refresh rate 75 Hz) following a 1.5-h warm-up period. Refractive correction was provided by a full aperture trial lens before the test eye, incorporating a subjectively refined near addition appropriate for the viewing distance of the monitor. The fellow eye was occluded with an opaque eye patch. The trial lens was placed at the anterior focal point of the eye (15.2 mm) to invoke Knapp's law,[45] thus minimising relative spectacle magnification and maintaining a near-constant retinal image size (in mm) for all participants. This step was seen as being important to minimise any potential optical factors on temporal summation such that any finding of altered temporal summation in myopia would be attributable to a neural origin.[46] The power of the trial lens was determined by non-cycloplegic objective refraction (Shin Nippon NVision-K 5001 binocular open field autorefractor, Shin-Nippon, grand seiko.com) and subjective refraction at a 6 m viewing distance. Astigmatism was corrected if >1.00 DC, otherwise the BVS lens was used. The position of the trial lens with regard to the eye was checked at regular intervals.

The display monitor had an achromatic background with a mean luminance of 10 cd/m^2. The maximum luminance of the test stimuli was 126.6 cd/m^2 and the chromaticity coordinates of both the background and stimuli were x = 0.258 and y = 0.257, as measured with a colorimeter (ColorCal-II Cambridge Research Systems, crsltd.com). All stimuli were generated in MATLAB (2016b, The MathWorks Inc., mathw orks.com) with Psychtoolbox (v3.0) and Bits-# (Cambridge Research Systems, crsltd.com). During experiments, participants were asked to fixate on a central white ring target (0.5° diameter) with a central negative contrast spot (0.25° diameter). Stimuli were presented at 10° eccentricity along

TABLE 1 Characteristics of the myopic and control groups.

	Controls (n = 21)	Myopes (n = 24)	Low -moderate myopes (n = 12)	High myopes (n = 12)
Age (years)	25.00 [22.00 to 40.00]	29.00 [24.50 to 40.50]	31.00 [24.00 to 47.00]	27.50 [24.50 to 40.00]
Refractive Error BVS (DS)	+1.00 [+0.25 to +1.38]	−4.50 [−2.50 to −6.25]	−2.50 [−2.00 to −3.88]	−6.25 [−5.50 to −8.25]
Astigmatism (DC)	−0.25 [0.00 to −0.63]	−0.88 [−0.50 to −1.38]	−0.75 [−0.50 to −1.25]	−1.00 [−0.50 to −1.50]
Axial length (mm)	23.59 [22.68 to 24.13]	25.38 [24.56 to 26.28]	24.77 [24.10 to 25.33]	26.18 [25.54 to 26.54]
Mean corneal curvature (mm)	7.78 [7.53 to 7.96]	7.64 [7.53 to 7.81]	7.59 [7.51 to 7.84]	7.65 [7.53 to 7.81]

Note: Summary values are presented as median [IQR].

Abbreviation: BVS, Best Vision Sphere.

the 90°, 180°, 270° and 360° meridians. Achromatic contrast thresholds were measured for a Goldmann III equivalent stimulus (0.43° diameter) of six different durations (1–15 frames, Bridgeman[47] duration: 1.1–187.8 ms).

Psychophysical procedure

All experimental measurements were carried out after the instillation of tropicamide hydrochloride 1.0%, with pupil diameter for all participants ≥6.5 mm following dilation. Contrast thresholds were measured for each of the six stimulus durations in six separate, randomly-ordered test runs. A 1–1 'YES-NO' staircase procedure was used to measure threshold. Stimulus contrast was varied in 0.5 log unit steps up to the first reversal, in 0.25 log unit steps until the second reversal, 0.1 log unit steps between reversals two and three and then by 0.05 log units until staircase termination. The staircase terminated after six reversals, with the final four reversals being used to calculate threshold.

Within each stimulus run, threshold was measured at the four test locations in a randomly interleaved fashion. The false positive rate was monitored by presenting 12 zero contrast stimuli, with tests rejected and repeated if the false positive rate was above 20%. Participant responses were collected with a Cedrus RB-540 response pad (Cedrus Corporation, cedrus.com). A response window of 2 s was permitted, and if no response was collected during this period, the stimulus was assumed to be unseen. Regular rest periods were provided at intervals throughout each data collection phase and when requested.

Estimating the critical duration from psychophysical measures

To account for spatial inhomogeneity of the CRT display, luminance values for the background and each stimulus step, measured at each location separately, were used in the calculation of the local contrast threshold. Contrast energy values (ΔE, in cd/m^2.s.deg^2) were calculated for each stimulus as the product of increment luminance (cd/m^2), stimulus duration (s) and stimulus area (deg^2) (Equation 1, where ΔL = increment luminance, f = number of frames within the stimulus, r = frame rate of the CRT (75 Hz) and A = stimulus area).

$$\Delta E = \Delta L . \frac{f}{r} . A \qquad (1)$$

The six stimuli were presented for 1, 2, 3, 5, 9 and 15 frames, respectively. Given a frame rate of 75 Hz, stimulus duration would be expected to range from 13.3 to 200 ms if expressed using the sum-of-frames (SOF) method (i.e., simply dividing the number of frames by the monitor frame rate). However, the SOF method can cause inaccuracies when using a CRT monitor as it assumes that the stimulus is presented for the whole frame duration, ignoring the well-known effects of phosphor decay. As such, it can lead to an overestimation of *true* stimulus duration for a CRT monitor, especially for short-duration stimuli. Previous work has demonstrated that using the SOF method to express stimulus duration on a CRT display can lead to an artefactual overestimation of the CD, with the magnitude of error being inversely related to frame rate.[48] To account for this, we, therefore, expressed stimulus durations using a modified version of the Bridgeman method,[47] which includes an adjustment for phosphor decay when calculating stimulus duration. This method quantifies stimulus duration as the point of phosphor activation in the first frame, to the end of phosphor activity in the final frame. The calculation of Bridgeman duration involves using the phosphor decay of the CRT monitor, which was measured using an Optical Transient Response Analyzer 3 (OTR-3, Display Metrology and Systems, GmbH & Co. KG, display-messtechnik.de), specified to 10% of the peak output in line with other studies that have used this technique.[35] This value (1.09 ×10^{-3} seconds) of phosphor persistence (p) was then used in Equation 2 together with the frame number (f) and monitor frame rate (r) to calculate the Bridgeman duration (tb) in seconds, for the six stimuli used in the study. The following Bridgeman durations were subsequently used in the study: 1.1, 14.4, 27.8, 54.4, 107.8 and 187.8 ms.

$$tb = \left(\frac{f-1}{r} \right) + p \qquad (2)$$

Temporal summation functions were then generated using the calculated contrast energy values and Bridgeman durations. A summation function was plotted for each test location, with the CD estimated with iterative two-phase regression analysis. This involves constraining the slope of the first line to zero to reflect Bloch's law (with a variable intercept) but allowing the slope and intercept of the second line to vary. The intersection of the two lines was taken as the CD. Data were excluded from further analysis if the software failed to estimate the CD (due to excessive variability in threshold measurements) or fit a segmented regression line to the data (i.e., the estimated CD was less than the shortest duration stimulus or greater than the maximum duration stimulus). An average CD was calculated for each participant from the locations where a CD estimate was gained. Summary temporal summation functions for both the myopic and control groups were produced using the median energy thresholds for the respective groups.

Biometric measurements: Ocular length

Axial and off-axis measurements of ocular length were obtained using an IOLMaster (Carl-Zeiss Meditec, zeiss.com) with a custom-built four-LED ring target fixed to the front of the instrument to enable the off-axis measurements. Measurements were taken axially, and at 10° along the 90°,

180°, 270° and 360° meridians to provide structural measurements co-localised to the functional measurements of temporal summation. Three measurements were taken at each position, and an average was calculated for each participant.

Structural measurements: Retinal ganglion cell number

The number of RGCs underlying the GIII stimulus was estimated for each participant using an OCT model method, based on the work of Raza and Hood[49] and the amendments proposed by Montesano et al.[50] This method was chosen rather than using measures of peripheral grating resolution acuity (PGRA) to estimate RGC density, as PGRA likely targets only the midget-RGC subtype, which may not be the RGC subtype activated by our functional measures of contrast thresholds.[51] In brief, the segmentation of individual B-scans was checked manually for accuracy by two experienced optometrists (VS, PJM). The OCT data were subsequently exported as RAW (.vol) files with the Heidelberg Eye Explorer (HEYEX) software. Using a custom MATLAB routine, an interpolated thickness map of the retinal ganglion cell layer (RGCL), the same size as the reference scanning laser ophthalmoscope retinal image (30° × 30°), was generated using the segmentations generated from the HEYEX software. If OCT data were unavailable, the thickness map was padded with zero values. The location of the anatomic fovea was identified through template matching but also checked manually for accuracy. A normative RGC volumetric density map (RGC/mm^3) was generated by dividing a normative histological map of RGC density[52] (RGC/mm^2) point-by-point by the mean RGCL thickness map (expressed in mm) in control observers. Individual RGC density maps were then generated by multiplying, point-by-point, the normative RGC volumetric density map (rotated according to each participant's fovea-optic nerve head axis and scaled according to the departure of each participant's axial length from that of the histology data,[53] [23.8 mm] assuming a global expansion model) with the RGCL thickness maps (mm) for each study participant. To ensure the histology and OCT maps were in common spatial units (mm), OCT scan data were corrected for axial length-induced image magnification with the abbreviated axial length method.[54]

To estimate the number of RGCs underlying each stimulus, the area and location of stimuli were first converted from degrees of visual space to mm on the retina with an eccentricity-specific conversion factor (q_p).[54] As Knapp's law was invoked during the functional measurements, a constant conversion factor was used for all participants assuming an emmetropic axial length of 23.84 mm.[53] Both the location and shape of each stimulus were subsequently corrected for the displacement of RGC bodies relative to the photoreceptor(s) projecting to them, using the method of Drasdo et al.,[55] with the amendments proposed by

Montesano et al.[50] RGC number underlying the stimulus was calculated with Equation 3, where RGCL is the participant's RGCL thickness (mm), GCD is the normative volumetric density values (RGC/mm^3) and S$_{area}$ (mm^2) is the retinal area of the stimulus:

$$RGC_{number} = RGCL \cdot GCD \cdot S_{area} \qquad (3)$$

Statistical analysis

Analysis was carried out in MATLAB (2019a, The MathWorks Inc., mathworks.com) and the freely available open-source statistical environment R (R Foundation for Statistical Computing, r-project.org). An alpha of 0.05 was considered the cut-off for statistical significance. In all cases, a Shapiro–Wilk test was used to determine if data sets followed a normal distribution, and the appropriate parametric or non-parametric statistical tests were applied accordingly. The Mann–Whitney U-Test was used to compare the CD between myopes and non-myopic controls. To investigate the relationship between functional measures of CD and co-localised structural parameters (ocular length, RGC number), ordinary least squares linear regression and Pearson's correlation were used. For all structure–function analysis, the logarithmic transform of both structural and functional data sets was undertaken.

RESULTS

A set of contrast thresholds for stimuli of different durations at an individual location is herein referred to as a temporal summation dataset. A total of 180 temporal summation datasets (96 in myopic participants and 84 in the non-myopic control group) were gathered across all locations and participants. Temporal summation datasets could not be fitted within the two-line regression model in 27 locations across all participants. Eighty datasets were successfully fitted with a two-phase regression line in the myopic group and 73 in the control group. From these remaining plots, an average CD was calculated for all participants (myopes $n = 24$, controls $n = 21$). There was no statistically significant difference ($p = 0.90$, Mann–Whitney U-test) in average CD between the myopic group (median: 44.3 ms; IQR: 26.5, 51.2) and the non-myopic group (median: 41.6 ms; IQR: 27.3, 48.5, Figure 1). There was also no statistically significant difference ($p = 0.64$, Mann–Whitney U test) in the average slope of the second line, representing the degree of partial or incomplete temporal summation exhibited, between the myopic group (median: 0.65; IQR: 0.49, 0.82) and the non-myopic group (median: 0.64; IQR: 0.54, 0.83).

While energy thresholds might seem higher in the myopia group compared with the control group for all stimulus durations (Figure 2), a mixed-model ANOVA found neither significant effect of the refractive group on energy thresholds ($p = 0.94$) nor an interaction between stimulus

duration and refractive group ($p=0.90$). Energy thresholds did, however, differ significantly as a function of stimulus duration ($p<0.001$). In addition, there was no relationship between stimulus duration and the difference in energy thresholds between myopes and controls (Pearson's $r=0.14$, $p=0.79$), supporting the finding that CD does not vary in myopia. Boxplots of thresholds for each stimulus duration are shown in Figure 2, together with summary temporal summation functions (based on median thresholds). Threshold data from locations where a temporal summation function could not be fitted successfully were excluded from the median calculations.

There was a significantly smaller ($p<0.001$) number of RGCs underlying the GIII-stimulus in the myopic group (median: 71.0; IQR: 62.4, 73.2) compared with the non-myopic group (median 81.5, IQR 76.7–87.6), and a significant, negative correlation between RGC number underlying the GIII stimulus and ocular length (Pearson's $r=-0.70$, $p<0.001$,

Figure 3). However, there was no relationship between CD estimates and either co-localised ocular length (Pearson's $r=-0.08$, $p=0.61$, Figure 4a) nor RGC number (Pearson's $r=-0.13$, $p=0.43$, Figure 4b).

DISCUSSION

We observed no significant difference in CD between myopes and non-myopic controls under low-photopic adaptation conditions. There was also no relationship between CD measures and either ocular length or RGC number underlying the GIII stimulus. In addition, there was no difference in partial summation between the two groups. As such, it appears that temporal summation remains unchanged in myopia despite structural differences between myopic and non-myopic retinae.

While no study, to our knowledge, has investigated temporal summation in myopia, previous work[5,7] has reported an enlarged area of complete spatial summation (RA) under the same conditions used in this study. Taken together, the findings of altered spatial summation but preserved temporal summation provides further insights as to the likely source of altered spatial summation in non-pathological myopia. In addition, there are important implications for our understanding of how glaucoma affects visual processing and how the disease may potentially be differentiated from physiological sources of altered RGC density. In the case of altered spatial summation in myopia, it has been hypothesised that such changes are a functional response to reduced RGC density (cells/mm^2), similar to the hypothesis proposed to account for the effects of both pathological (e.g., glaucoma[39]) and physiological (e.g., retinal eccentricity[56–58]) alterations in RCG density on spatial summation. Specifically, it has been suggested that where RGC density is reduced, RA is enlarged to recruit responses from a constant number of RGCs to optimise overall neural sensitivity at the expense of spatial resolution.[39,58] In contrast to glaucoma, temporal summation is unaffected by
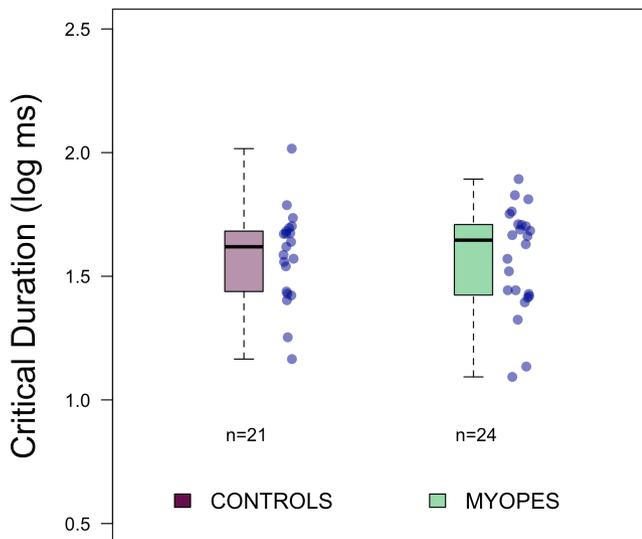

FIGURE 1 Average critical duration measured for individual myopic and non-myopic control participants. Individual data points are represented by blue dots.
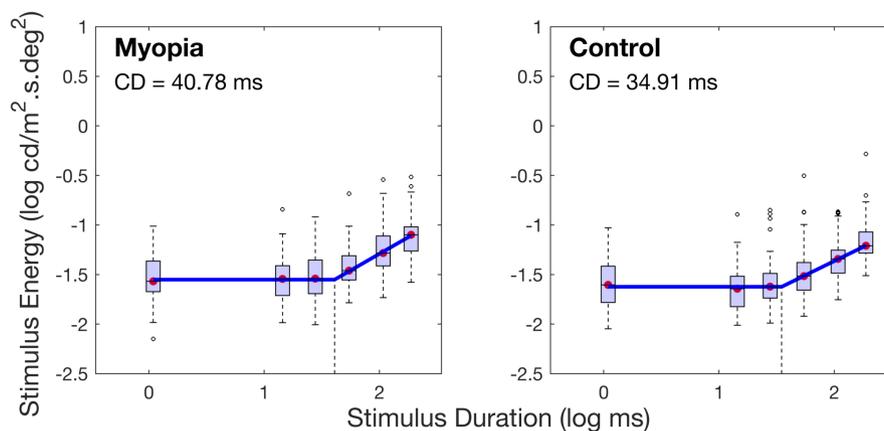

FIGURE 2 Summary temporal summation functions based on median thresholds for both the myopia and control groups. The position and spread of energy thresholds for each group are represented by box and whisker plots.

both refractive error (this study) and retinal eccentricity[59] when measured using a GIII stimulus in control observers.

In the case of altered temporal summation in glaucoma, it has been proposed that changes in RGC density and also pre-morbid dysfunction in remaining cells underpin the observed changes.[35] This hypothesis is supported by the fact that residual deficits in temporal summation were found even after changes in spatial summation (i.e., RGC density) were accounted for. With this in mind, altered spatial summation in axial myopia, without accompanying changes in temporal summation, would point to reduced RGC density (as would be expected due to retinal stretching) but without dysfunction within the cells themselves. This agrees with our previous finding where differences in spatial summation between myopes and non-myopes were no longer apparent when retinal image size was allowed
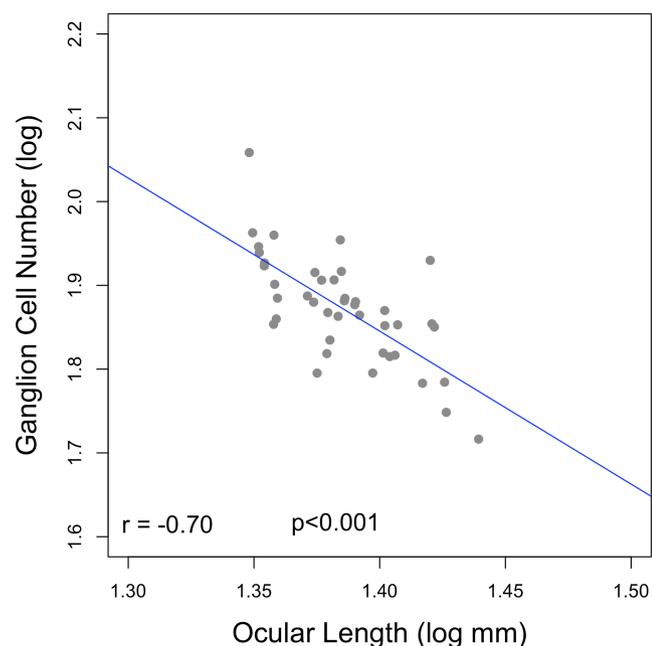
to vary with axial length.[7] The larger retinal image size in myopia appeared to offset completely the reduced RGC density. In other words, for the same nominal stimulus size, the area of coverage on the retina enlarged due to magnification at the same rate as retinal stretching, encompassing a constant number of RGCs and leaving no apparent change in visual function. Optimisation of visual function through the use of a contact lens correction in high myopia may also lend support to this hypothesis.[60,61] Other studies have also found that the enlarged retinal image size in axial myopia compensates for the more widely spaced neural elements in measurements of spatial visual function.[2,5,40]

While it appears that altered RGC density and/or function plays a central role in moderating physiological and pathological changes in spatiotemporal summation, further research is necessary to identify what role cortical processing plays in moderating such functional changes. For example, it has been hypothesised that RA is determined by the spatial extent of the cortical filter that receives input from ~31 RGCs under the adaptation conditions used in this study.[62] Within the visual cortex there could be many different filters of varying spatial frequency, with RA determined by the 'dominant' cortical filter, which is the cortical filter that receives input from 31 RGCs. As RGCs are lost in glaucoma or become sparser with retinal eccentricity or with myopic retinal stretch, then the cortical filter now receiving input from 31 RGCs would be larger (i.e., a filter that originally received signals from >31 RGCs, once the RGC number drops now only receives input from 31 and thus became the 'dominant' or most highly-weighted filter), with the overarching result that RA would increase in size.[39]

Figure S1 shows the CD data for this study plotted alongside the results for glaucoma participants from Mulholland et al.[35] That temporal summation is unaffected by myopia, but altered in glaucoma,[35] suggests that probing deficits in temporal summation could enable greater diagnostic accuracy when attempting to differentiate glaucoma-related RGC damage/loss (i.e., pathological change) from alterations in RGC density related to axial myopia (i.e.,

FIGURE 3 Relationship between retinal ganglion cell number underlying the Goldmann GIII stimulus and ocular length.
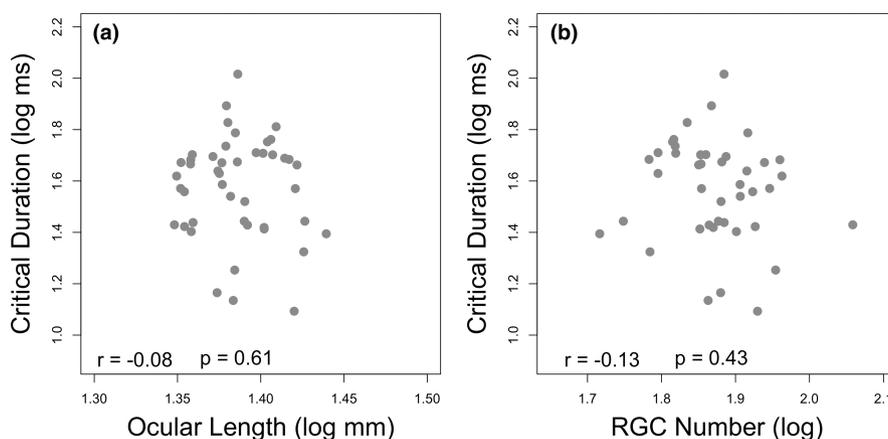

FIGURE 4 Critical duration plotted against (a) ocular length and (b) retinal ganglion cell (RGC) number underlying Goldmann GIII stimulus.

physiological variation). While measuring temporal summation psychophysically to obtain an individual's CD is unrealistic in a clinical setting, given the requirement for a dedicated psychophysical set-up and prolonged testing time, these known deficits in temporal processing in glaucoma (compared with myopia) could potentially be exploited by novel perimetric stimuli which have a duration that is shorter than the CD in healthy observers.[63]

Currently, many clinical measures of structure or function are not capable of effectively differentiating glaucoma-related alterations from physiological myopic changes when analysed cross-sectionally.[64–67] For example, in myopia the optic nerve head can be surrounded by peripapillary atrophy[68,69] with reductions in OCT-derived RNFL thickness.[32,70–76] These structural changes are also typically observed in glaucoma. Functional deficits can also present in myopia, in the form of visual field defects[65,77–79] and overall reductions in visual field sensitivity in the absence of glaucoma.[65,80] For example, Aung et al.[80] reported a reduction in the mean deviation (MD) by 0.20 dB for every dioptre of myopia above 4.00 D. Ding et al.[65] also found that 16% of their highly myopic sample (Chinese participants aged 7–70 years, median age 17.4 years) had visual field defects that mimicked classic glaucomatous defects (nasal step, arcuate), with 3% exhibiting dense arcuate defects characteristic of moderate to advanced glaucoma. The similarity between the functional abnormalities resulting from myopia and glaucoma was also highlighted by Chang and Singh.[66]

Given that cross-sectional analysis of both structural and functional clinical tests in myopia can mimic glaucoma, longitudinal measurements may be required to distinguish glaucomatous from non-glaucomatous alterations in RGC density in myopes with currently available technology. This can hinder the detection of glaucoma in myopic individuals, with associated burdens for both patients (e.g., increased patient anxiety) and healthcare systems (e.g., overuse of valuable clinic time and resources). A method that is capable of cross-sectionally differentiating between glaucoma-related visual function deficits and those resulting from myopia would, therefore, be very beneficial. Given the findings of the current study, scaling the duration of the stimulus used in perimetry to be within the local CD in a healthy population could enable greater cross-sectional differentiation between glaucoma-related visual function deficits and those related to myopia. This approach would also be beneficial for the detection of glaucoma onset and progression, with Mulholland et al.[35] calculating that the glaucoma disease signal could be boosted by ~200% compared with the current GIII/200 ms stimulus if the anomalies in temporal summation in glaucoma are targeted in this way. Once a more appropriate novel perimetric stimulus has been selected, this should be used in combination with better statistical methods to optimise the detection of glaucoma progression.

While this study investigated temporal summation in myopia using a GIII-sized stimulus to align with clinical perimetric strategies, Owen hypothesised that true complete temporal summation may only occur if the stimulus is smaller than RA.[33] Even though RA generally enlarges with myopia, this may not have been the case for all participants. As such, future work should also investigate temporal summation in myopia using a stimulus scaled to the localised RA within an individual (i.e., under conditions of complete spatial summation).

CONCLUSIONS

No change in temporal summation was observed in participants with myopia compared with non-myopic controls, despite a previous finding of altered spatial summation under identical experimental conditions.[7] This indicates that although RGC density (cells/mm^2) changes in myopia, RGC function does not. Given that temporal summation is altered in glaucoma, but not in myopia, perimetric strategies optimised to identify deficits in temporal summation may improve the accuracy with which glaucoma-related visual deficits due to RGC loss and/or pre-morbid dysfunction may be differentiated from myopia-related changes in visual function due to altered RGC density.

ORCID
Victoria Stapley https://orcid.org/0000-0001-7486-4125

Roger S. Anderson https://orcid.org/0000-0003-3981-707X
Tony Redmond https://orcid.org/0000-0002-6997-5231
Kathryn Saunders https://orcid.org/0000-0002-9289-5731
Pádraig J. Mulholland https://orcid.org/0000-0001-5166-0592

REFERENCES

1. Strang NC, Winn B, Bradley A. The role of neural and optical factors in limiting visual resolution in myopia. *Vision Res*. 1998;38:1713–21.
2. Coletta NJ, Watson T. Effect of myopia on visual acuity measured with laser interference fringes. *Vision Res*. 2006;46:636–51.
3. Wolsley CJ, Saunders KJ, Silvestri G, Anderson RS. Investigation of changes in the myopic retina using multifocal electroretinograms, optical coherence tomography and peripheral resolution acuity. *Vision Res*. 2008;48:1554–61.
4. Chui TYP, Yap MKH, Chan HHL, Thibos LN. Retinal stretching limits peripheral visual acuity in myopia. *Vision Res*. 2005;45:593–605.
5. Atchison DA, Schmid KL, Pritchard N. Neural and optical limits to visual performance in myopia. *Vision Res*. 2006;46:3707–22.
6. Liou S-W, Chiu C-J. Myopia and contrast sensitivity function. *Curr Eye Res*. 2001;22:81–4.
7. Stapley V, Anderson RS, Saunders KJ, Mulholland PJ. Altered spatial summation optimizes visual function in axial myopia. *Sci Rep*. 2020;10:12179. https://doi.org/10.1038/s41598-020-67893-8
8. Rossi EA, Weiser P, Tarrant J, Roorda A. Visual performance in emmetropia and low myopia after correction of high-order aberrations. *J Vis*. 2007;7:14. https://doi.org/10.1167/7.8.14
9. Ehsaei A, Chisholm CM, Pacey IE, Mallen EAH. Visual performance fall-off with eccentricity in myopes versus emmetropes. *J Optom*. 2013;6:36–44.
10. Pan F, Swanson WH. A cortical pooling model of spatial summation for perimetric stimuli. *J Vis*. 2006;6:1159–71.
11. Redmond T, Zlatkova M, Vassilev A, Garway-Heath D, Anderson RS. Changes in Ricco's area with background luminance in the S-cone pathway. *Optom Vis Sci*. 2013;90:66–74.
12. Je S, Ennis FA, Woodhouse JM, Sengpiel F, Redmond T. Spatial summation across the visual field in strabismic and anisometropic amblyopia. *Sci Rep*. 2018;8:3858. https://doi.org/10.1038/s41598-018-21620-6
13. Witkovsky P. Dopamine and retinal function. *Doc Ophthalmol*. 2004;108:17–40.
14. Ong J, Wong T. Effect of ametropias on critical fusion frequency. *Am J Optom Arch Am Acad Optom*. 1971;48:736–9.
15. Chen PC, Woung LC, Yang CF. Modulation transfer function and critical flicker frequency in high-myopia patients. *J Formos Med Assoc*. 2000;99:45–8.
16. Comerford JP, Thorn F, Corwin TR. Effect of luminance level on contrast sensitivity in myopia. *Am J Optom Physiol Opt*. 1987;64:810–4.
17. Vera-Diaz FA, Bex PJ, Ferreira A, Kosovicheva A. Binocular temporal visual processing in myopia. *J Vis*. 2018;18:17. https://doi.org/10.1167/18.11.17
18. Yamamoto S, Nitta K, Kamiyama M. Cone electroretinogram to chromatic stimuli in myopic eyes. *Vision Res*. 1997;37:2157–9.
19. Chan H, Mohidin N. Variation of multifocal electroretinogram with axial length. *Ophthalmic Physiol Opt*. 2003;23:133–40.
20. Sachidanandam R, Ravi P, Sen P. Effect of axial length on full-field and multifocal electroretinograms. *Clin Exp Optom*. 2017;100:668–75.
21. Koh V, Tan C, Nah G, Zhao P, Yang A, Lin ST, et al. Correlation of structural and electrophysiological changes in the retina of young high myopes. *Ophthalmic Physiol Opt*. 2014;34:658–66.
22. Perlman I, Meyer E, Haim T, Zonis S. Retinal function in high refractive error assessed electroretinographically. *Br J Ophthalmol*. 1984;68:79–84.
23. Ishikawa M, Miyake Y, Shiroyama N. Focal macular electroretinogram in high myopia. *Nippon Ganka Gakkai Zasshi*. 1990;94:1040–7.
24. Westall CS, Dhaliwal HM, Panton C, Sigesmund D, Levin A, Nischal K, et al. Values of electroretinogram responses according to axial length. *Doc Ophthalmol*. 2001;102:115–30.
25. Hidajat R, Mclay J, Burley C, Elder M, Morton J, Goode D. Influence of axial length of normal eyes on PERG. *Doc Ophthalmol*. 2003;107:195–200.
26. Luu CD, Foulds WS, Tan DTH. Features of the multifocal electroretinogram may predict the rate of myopia progression in children. *Ophthalmology*. 2007;114:1433–8.
27. Kawabata H, Adachi-Usami E. Multifocal electroretinogram in myopia. *Invest Ophthalmol Vis Sci*. 1997;38:2844–51.
28. Luu CD, Lau AI, Lee S. Multifocal electroretinogram in adults and children with myopia. *Arch Ophthalmol*. 2006;124:328–34.
29. Kader MA. Electrophysiological study of myopia. *Saudi J Ophthalmol*. 2012;26:91–9.
30. Park S, Kim SH, Park TK, Ohn YH. Evaluation of structural and functional changes in non-pathologic myopic fundus using multifocal electroretinogram and optical coherence tomography. *Doc Ophthalmol*. 2013;126:199–210.
31. Song AP, Yu T, Wang JR, Liu W, Sun Y, Ma SX. Multifocal electroretinogram in non-pathological myopic subjects: correlation with optical coherence tomography. *Int J Ophthalmol*. 2016;9:286–91.
32. Ismael ZF, El-Shazly AAE, Farweez YA, Osman MMM. Relationship between functional and structural retinal changes in myopic eyes. *Clin Exp Optom*. 2017;100:695–703.
33. Owen WG. Spatio-temporal integration in the human peripheral retina. *Vision Res*. 1972;12:1011–26.
34. Rogers J, Chauhan BC, Leblanc RP. Temporal summation in glaucoma patients and normal controls using high-pass resolution stimuli. *Invest Ophthalmol Vis Sci*. 1994;35:4326–96.
35. Mulholland PJ, Redmond T, Garway-Heath DF, Zlatkova MB, Anderson RS. Spatiotemporal summation of perimetric stimuli in early glaucoma. *Invest Ophthalmol Vis Sci*. 2015;56:6473–82.
36. Bloch AM. Experiences sur la vision. *CR Soc Biol Paris*. 1885;37:493–5.
37. Kietzman ML, Gillam BJ. Visual temporal integration and simple reaction time. *Percept Psychophys*. 1972;11:333–40.
38. Barlow HB. Temporal and spatial summation in human vision at different background intensities. *J Physiol*. 1958;141:337–50.
39. Redmond T, Garway-Heath DF, Zlatkova MB, Anderson RS. Sensitivity loss in early glaucoma can be mapped to an enlargement of the area of complete spatial summation. *Invest Ophthalmol Vis Sci*. 2010;51:6540–8.
40. Nagra M, Gilmartin B, Logan NS, Anderson SJ. The effects of severe myopia on the properties of sampling units in peripheral retina. *Optom Vis Sci*. 2018;95:399–404.
41. Jiang X, Xu Z, Soorma T, Tariq A, Bhatti T, Baneke AJ, et al. Electrical responses from human retinal cone pathways associate with a common genetic polymorphism implicated in myopia. *Proc Natl Acad Sci U S A*. 2022;119:e2119675119. https://doi.org/10.1073/pnas.2119675119
42. Hartline HK. Intensity and duration in the excitation of single photoreceptor units. *J Cell Comp Physiol*. 1934;5:229–47.
43. Rosenblum RA. Electroretinographic evaluation of the Bunsenroscoe law for the human eye at high energy levels. *Invest Ophthalmol*. 1971;10:904–10.
44. World-Health-Organization. The impact of myopia and high myopia. 2015.
45. Knapp H. The influence of spectacles on the optical constant and visual acuteness of the eye. *Arch Ophthalmol*. 1869;1:377–410.
46. Mulholland PJ, Redmond T, Garway-Heath DF, Zlatkova MB, Anderson RS. The effect of age on the temporal summation of achromatic perimetric stimuli. *Invest Ophthalmol Vis Sci*. 2015;56:6467–72.
47. Bridgeman B. Durations of stimuli displayed on video display terminals: (n − 1)/f + persistence. *Psychol Sci*. 1998;9:232–3.
48. Mulholland PJ, Zlatkova MB, Redmond T, Garway-Heath DF, Anderson RS. Effect of varying CRT refresh rate on the measurement of temporal summation. *Ophthalmic Physiol Opt*. 2015;35:582–90.

49. Raza AS, Hood DC. Evaluation of the structure-function relationship in glaucoma using a novel method for estimating the number of retinal ganglion cells in the human retina. *Invest Ophthalmol Vis Sci*. 2015;56:5548–56.

50. Drasdo N, Millican CL, Katholi CR, Curcio CA. The length of Henle fibers in the human retina and a model of ganglion receptive field density in the visual field. *Vision Res*. 2007;47:2901–11.

51. Stapley V, Anderson RS, Saunders K, Mulholland PJ. Examining the concordance of retinal ganglion cell counts generated using measures of structure and function. *Ophthalmic Physiol Opt*. 2022;42:1338–52.

52. Curcio CA, Allen KA. Topography of ganglion cells in human retina. *J Comp Neurol*. 1990;300:5–25.

53. Curcio CA, Sloan KR, Meyers D. Computer methods for sampling, reconstruction, display and analysis of retinal whole mounts. *Vision Res*. 1989;29:529–40.

54. Bennett AG, Rudnicka AR, Edgar DF. Improvements on Littmann's method of determining the size of retinal features by fundus photography. *Graefes Arch Clin Exp Ophthalmol*. 1994;232:361–7.

55. Montesano G, Ometto G, Hogg RE, Rossetti LM, Garway-Heath DF, Crabb DP. Revisiting the Drasdo model: implications for structure-function analysis of the macular region. *Transl Vis Sci Technol*. 2020;9:15. https://doi.org/10.1167/tvst.9.10.15

56. Fischer B. Overlap of receptive field centers and representation of the visual field in the cat's optic tract. *Vision Res*. 1973;13:2113–20.

57. Volbrecht V, Shrago EE, Schefrin BE, Werner J. Spatial summation in human cone mechanisms from 0 degrees to 20 degrees in the superior retina. *J Opt Soc Am A*. 2000;17:641–50.

58. Kwon M, Liu R. Linkage between retinal ganglion cell density and the nonuniform spatial integration across the visual field. *Proc Natl Acad Sci U S A*. 2019;116:3827–36.

59. Mulholland P, Redmond T, Zlatkova M, Garway-Heath D, Anderson R. Temporal summation varies with visual field eccentricity for perimetric stimuli scaled to the area of complete spatial summation. *ARVO E-Abstract*. 2013;54:3924.

60. Bradley A, Rabin J, Freeman RD. Nonoptical determinants of aniseikonia. *Invest Ophthalmol Vis Sci*. 1983;24:507–12.

61. Rabin J, Bradley A, Freeman RD. On the relation between aniseikonia and axial anisometropia. *Am J Optom Physiol Opt*. 1983;60:553–8.

62. Swanson WH, Felius J, Pan F. Perimetric defects and ganglion cell damage: interpreting linear relations using a two-stage neural model. *Invest Ophthalmol Vis Sci*. 2004;45:466–72.

63. Mulholland PJ, Redmond T, Garway-Heath DF, Zlatkova MB, Anderson RS. Estimating the critical duration for temporal summation of standard achromatic perimetric stimuli. *Invest Ophthalmol Vis Sci*. 2015;56:431–7.

64. Yamashita T, Asaoka R, Tanaka M, Kii Y, Yamashita T, Nakao K, et al. Relationship between position of peak retinal nerve fiber layer thickness and retinal arteries on sectoral retinal nerve fiber layer thickness. *Invest Ophthalmol Vis Sci*. 2013;54:5481–8.

65. Ding X, Chang RT, Guo X, Liu X, Johnson CA, Holden BA, et al. Visual field defect classification in the Zhongshan ophthalmic center-Brien Holden vision institute high myopia registry study. *Br J Ophthalmol*. 2016;100:1697–702.

66. Chang RT, Singh K. Myopia and glaucoma: diagnostic and therapeutic challenges. *Curr Opin Ophthalmol*. 2013;24:96–101.

67. Nitta K, Sugiyama K, Wajima R, Tachibana G. Is high myopia a risk factor for visual field progression or disk hemorrhage in primary open-angle glaucoma? *Clin Ophthalmol (Auckland, NZ)*. 2017;11:599–604.

68. Kim TW, Kim M, Weinreb RN, Woo SJ, Park KH, Hwang JM. Optic disc change with incipient myopia of childhood. *Ophthalmology*. 2012;119:21–6.e1-3.

69. Fan YY, Jonas JB, Wang YX, Chen CX, Wei WB. Horizontal and vertical optic disc rotation. The Beijing eye study. *PLoS One*. 2017;12:e0175749. https://doi.org/10.1371/journal.pone.0175749

70. Leung CK, Mohamed S, Leung KS, Cheung CY, Chan SL, Cheng DK, et al. Retinal nerve fiber layer measurements in myopia: an optical coherence tomography study. *Invest Ophthalmol Vis Sci*. 2006;47:5171–6.

71. Budenz DL, Anderson DR, Varma R, Schuman J, Cantor L, Savell J, et al. Determinants of normal retinal nerve fiber layer thickness measured by stratus OCT. *Ophthalmology*. 2007;114:1046–52.

72. Rauscher FM, Sekhon N, Feuer WJ, Budenz DL. Myopia affects retinal nerve fiber layer measurements as determined by optical coherence tomography. *J Glaucoma*. 2009;18:501–5.

73. Kim MJ, Lee EJ, Kim TW. Peripapillary retinal nerve fibre layer thickness profile in subjects with myopia measured using the stratus optical coherence tomography. *Br J Ophthalmol*. 2010;94:115–20.

74. Wang G, Qiu KL, Lu XH, Sun LX, Liao XJ, Chen HL, et al. The effect of myopia on retinal nerve fibre layer measurement: a comparative study of spectral-domain optical coherence tomography and scanning laser polarimetry. *Br J Ophthalmol*. 2011;95:255–60.

75. Yuan YZ, Feng CL, Li BY, Shen MQ, Chen XP, Zhang CH, et al. The relationship between visual field global indices and retinal nerve fiber layer thickness in healthy myopes. *J Ophthalmol*. 2014;2014:431901. https://doi.org/10.1155/2014/431901

76. Mashige KP, Oduntan OA. Retinal nerve fibre layer thickness values and their associations with ocular and systemic parameters in black South Africans. *Afr Health Sci*. 2016;16:1188–94.

77. Fledelius HC, Goldschmidt E. Eye shape and peripheral visual field recording in high myopia at approximately 54 years of age, as based on ultrasonography and Goldmann kinetic perimetry. *Acta Ophthalmol*. 2010;88:521–6.

78. Ohno-Matsui K, Shimada N, Yasuzumi K, Hayashi K, Yoshida T, Kojima A, et al. Long-term development of significant visual field defects in highly myopic eyes. *Am J Ophthalmol*. 2011;152:256–65.e1.

79. Peric S, Cerovski B, Peric P, Skegro I, Tiljak H. Automated static perimetry: the influence of myopic anisometropia on evaluation of visual field. *Coll Antropol*. 2013;37(Suppl 1):75–81.

80. Aung T, Foster PJ, Seah SK, Chan SP, Lim WK, Wu HM, et al. Automated static perimetry: the influence of myopia and its method of correction. *Ophthalmology*. 2001;108:290–5.

SUPPORTING INFORMATION

Additional supporting information can be found online in the Supporting Information section at the end of this article.